Development of coupled optical techniques for the measurements of soot and precursors in laboratory flame and aero-engine technical combustors

Jean-Pierre Dufitumukiza, Nicolas Fdida, Klaus Peter Geigle, Zhiyao Yin, Axel Vincent, Rafael Barrellon-Vernay, Arnaud Ristori, David Carru, Pascal Cherubini, Daniel Gaffie, et al.

HAL Id: hal-03027439

https://hal.science/hal-03027439

Submitted on 4 Dec 2020

Development of coupled optical techniques for the measurements of soot and precursors in laboratory flame and aero-engine technical combustors

DUFITUMUKIZA Jean-Pierre[1,2], FDIDA Nicolas[1], GEIGLE Klaus Peter[3], YIN Zhiyao[3], VINCENT Axel[1], BARRELLON-VERNAY Rafael[1,4], RISTORI Arnaud[1], CARRU David[1], CHERUBINI Pascal[1], GAFFIE Daniel[1], MOHAMED Ajmal Khan[1], MERCIER Xavier[3], IRIMIEA Cornelia[1]

[1]DMPE, ONERA, Paris-Saclay Univ., Palaiseau, 91120, France, [2]Lille Univ., CNRS, PC2A, Villeneuve d'Ascq, 59655, France, [3]German Aerospace Center, Stuttgart, 70569, Germany, [4]Lille Univ., CNRS, PHLAM, Villeneuve d'Ascq, 59655, France

Main corespondence authors: jean-pierre.dufitumukiza@onera.fr, cornelia.irimiea@onera.fr

Abstract

This work is focused on the development of planar in-situ laser-based methods serving for the mapping of soot precursors and soot particles in hash combustion conditions. We target the soot molecular precursors and particulates because there are still unanswered questions related to the mechanisms leading to the formation of soot particles and their quantification in harsh combustion conditions. Laser-induced incandescence (LII) at 1064 nm is coupled with laser-induced fluorescence (LIF) at 532 nm to monitor soot and its precursors, respectively, on the MICADO test rig. A progressive approach is followed to implement the optical techniques, where LII/LIF is first tested and evaluated in a laminar diffusion flame, stabilized on a coflow burner at atmospheric pressure. Measurements of soot volume fraction and soot precursors are reported in combustion conditions similar to the cruise cycle in terms of total mass flow rate and pressure into the combustor.

Keywords: soot, polycyclic aromatic precursors, laser induced incandescence/fluorescence, harsh combustion conditions, nucleation, aeronautic combustor

1   Introduction

Combustion impacts many aspects of our life, including air quality and the use of energy sources[1–10]. Outstanding progress towards cleaner combustion has been achieved due to the development of lasers and fast acquisition systems and, nonetheless, due to the increased processing power of computers[11–17]. Despite these advancements, the characterization of the phenomena taking place in industrial-scale combustors is scarce due to the harsh combustion conditions and the difficulty to access at 'the core' of these complex systems[11,18–20]. On these grounds, there is a growing demand for the coupling of non-intrusive optical techniques that can provide several experimental parameters simultaneously with intrusive techniques for obtaining the maximum of information about the combustion phenomena, especially on the formation of gas and particulate emissions. These parameters may be used either as an input of theoretical models or to predict system failures as combustion instabilities, flame extinction, and uncontrolled emissions[21–24].

Aero-combustor testing requires facilities that are capable of simulating aero-thermodynamic conditions at the inlet of the combustion chamber (i.e. downstream from the compressor)[19]. Chamber pressure, inlet temperature and injection systems global equivalence ratios are the governing parameters to be respected for a representative simulation of the combustion chemical reactions inside the combustor. To answer this matter, ONERA and DLR are equipped with test rigs that have the capability and particularity of operating at working conditions similar (input airflow and pressure) to the ones found in aircraft engines[19,25]. This work presents non-intrusive optical techniques that characterize harsh combustion conditions, similar to those encountered in daily industrial applications. A joint experimental campaign between ONERA and DLR took place in the framework of the SOPRANO project[26]. The project goal is to reduce gaseous pollutants and soot particles in aero-engine combustors. Within this purpose, adapted optical techniques were used to measure and characterize particulate matter and gas emissions on a newly developed industrial test rig chamber - MICADO[19]. Notably, this work focused on implementing suitable planar in-situ laser-based methods for mapping soot precursors and soot particles into the MICADO combustion chamber equipped with optical access. Soot molecular precursors and particulates are targeted because there are still unanswered questions about the soot particles' formation and quantification mechanisms. Academic burners are used to develop optical techniques and study the mechanisms leading to soot formation in simple combustion conditions. In this study, an atmospheric pressure burner was used to stabilize a CH_4 laminar diffusion flame, containing soot and soot precursors. This burner was used to set up suitable optical techniques in terms of detection and synchronization. Laser induced incandescence (LII) and laser induced fluorescence (LIF) were implemented and developed for the simultaneous detection of soot and classes of polycyclic aromatic hydrocarbons (PAH) considered soot precursors[15,22,25,27,28]. These tests lead to the implementation of coupled LII/LIF on MICADO test rig for the study of combustion of kerosene with air in a pressure domain spanning the range 6 to 10 bar. Maps of soot and its precursors were obtained for combustion conditions representative of the cruise cycle in terms of pressure and air mass flow rate. LII was used to obtain soot cartography and LIF provided additional details on the processes involved in the nucleation of soot. The coupling of LIF with LII is appealing, especially in harsh combustion conditions. The gathered information is of

particular importance for these (technical) combustion conditions since they are not accessible in laboratory-scale experiments. Therefore, their such correlation provides a better understanding of phenomena taking place in technical gas turbine combustors.

2   Experimental setup: burners and optical techniques

In-situ planar LII and LIF were implemented on an academic burner at atmospheric pressure for initial configuration. MICADO test rig working at different working points was subject to in-situ measurements of coupled LII/LIF. MICADO test rig facility has been described in a previous publication and only a few details are presented here[19]. LII is a seldom-used technique to evaluate soot volume fractions. It has been applied to study soot particle formation and quantification in aero-engine test rigs by Geigle et al.[15,25]. LIF of soot precursors has been used to determine molecular compounds participating in soot nucleation in academic burners. The application of LIF at an industrial scale is scarce due to the high number of parameters affecting the combustion, the difficulty of being quantitative and selective for one molecular compound only[27,29,30].

2.1 Academic burner and MICADO test rig
2.1.1 Academic burner

A coaxial laboratory burner supplied with methane is used to study the soot formation processes (growth) in a laminar diffusions flame at atmospheric pressure. Additionally, this system is used to develop optical techniques adapted to the study of combustion conditions in industrial test rigs with limited access. A schematic representation of the coflow burner is presented in **Figure 1.a**. The laminar diffusion flame was stabilized with 16 L/min of air shield and 0.6 L/min of CH_4. These conditions resulted in a laminar flame with a height of 120 mm and 9 mm diameter near the injector. The flame was slightly flickering due to the configuration of the injector. A stabilization plate was used on the top of the flame in order to stabilize the flow fields. The burner has a central ceramic injector for the fuel with an outer diameter of 38 mm and an inner diameter of 6 mm. The diameter of the outer air co-flow tube is 63 mm. For the airflow homogenization, the empty volume surrounding the central injector was filled with glass beads placed on a layer of sintered material. The outer co-flow tube is supplied with compressed air using three injection points spaced at 120^0 at the burner base. Small flame perturbations were observed during the measurements, likely due to air currents formed into the laboratory or buoyancy forces.

2.1.2 MICADO test rig

MICADO test rig is a newly developed combustion facility equipped with an optical laboratory that allows the implementation of various techniques to study realistic conditions for the pressure and total air mass flow in the combustor[19]. Technical details of the test rig have been presented by Cochet et al.[19]. Only significant changes regarding the combustion parameters and the studied region of interest (ROI) are mentioned here.

The combustion chamber has a 100 mm x 100 mm square section, equipped with three optical access windows (89 mm x 88 mm), from which two are placed on the sides and one on the bottom. Air and fuel are fed to the combustor through an axial swirl injector. Fuel is injected either in main (premixed) or pilot (non-premixed) regimes. The fuel is ignited with a torch

placed on the upper side of the water-cooled combustor. The MICADO test facility operation range is: from 0.2 to 2.60 kg/s for the air mass, from 250 to 800 K for the air temperature, from 0.1 to 2.8 MPa for the pressure into the chamber. The chamber pressure is adjusted through an exit nozzle equipped with a throttling plug. The combustor can operate with gas or liquid fuel (methane or kerosene) at values below 100 g·s^{-1} for each injection line. A sampling probe allows online gas and/or soot analysis (sampling location at 140 mm downstream of the combustor dome). The fuel and airflow exit planes are located at the combustion chamber inlet and are defined as the zero position. A two mm metallic shield is hindering the optical access near the injector, as displayed **Figure 1. b**.
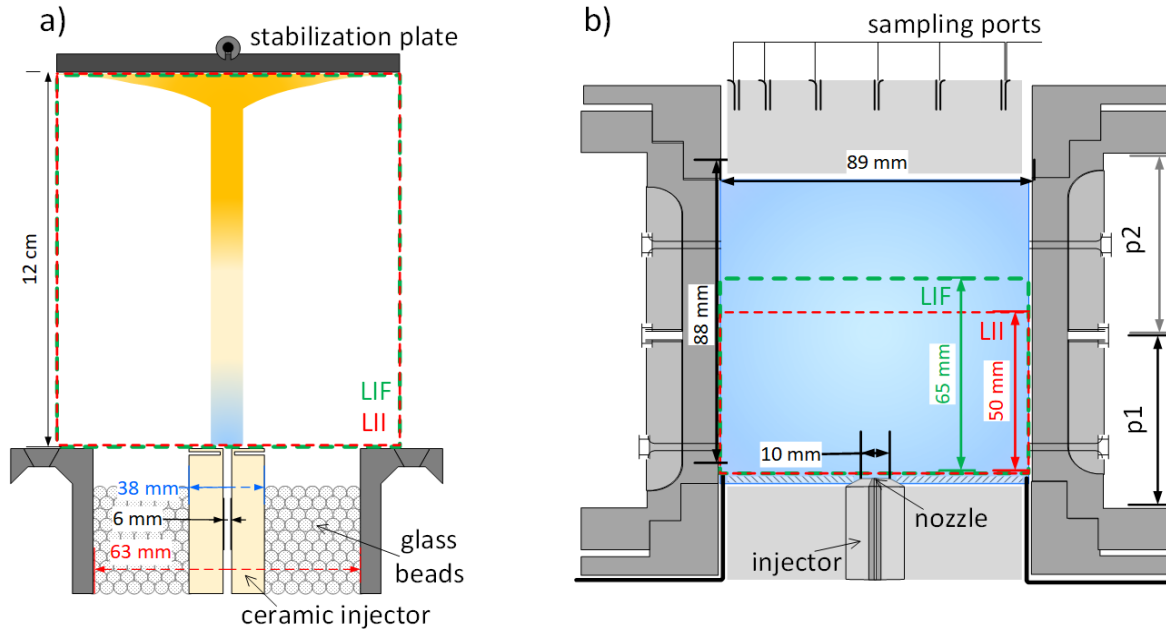

Figure 1. a) Academic coflow burner with the laminar diffusion flame and stabilization plate; **b)** The geometrical configuration of the MICADO test rig combustion chamber.

Multiple working points (WP) were tested during the joint sampling campaign. Three distinctive WP are selected for this work. Parameters as the pressure into the chamber (p_{ch}), the air temperature (T_{air}), the mass of air ($\dot{m}_{air}$), the mass of kerosene for the pilot ($\dot{m}_{pilot}$) or main ($\dot{m}_{main}$) injection, the global equivalence ratio (Φ), and the ration between the pilot and main injection are shown in **Table 1**.

working point	p_{ch} (MPa)	T_{air} (K)	$\dot{m}_{air}$ (kg/s)	$\dot{m}_{pilot}$ (kg/s)	$\dot{m}_{main}$ (kg/s)	Δp_{pilot} (bar)	Δp_{main} (bar)	Φ	pilot:main
WP 1	0.785	548	0.486	0.0234	0.0000	37.99	0.41	0.704	100:0
WP 2	1.008	544	0.250	0.0135	0.0000	12.93	0.29	0.788	100:0
WP 3	0.714	547	0.336	0.0099	0.0084	7.31	1.14	0.796	54:46

Table 1 Experimental parameters used to study the combustion conditions of kerosene with air. p_{ch} – pressure combustion chamber, T_{air} – injected air temperature, $\dot{m}_{air}$ – the total mass of air, $\dot{m}_{pilot}$ – the total mass of fuel injected in pilot mode, $\dot{m}_{main}$ - the total mass of fuel injected in main mode, Δp_{pilot} – differential pressure used for pilot injection, Δp_{main} – differential pressure used for the main injection, Φ – the estimated local equivalence ratio before injection, pilot:main – the ration between main and pilot injection.

All parameters were changed for the three WP, except the air temperature, which was kept constant to ~550 K. The pressure in the combustion chamber was set between 0.714 and 1.008 MPa. Two WP are characterized by pilot injection, while one WP is specific to pilot and main injection.

The laser sheet covered the entire ROI of the academic burner (120 mm), **Figure 1.a**. Two positions (p1 and p2) were selected to cover the entire MICADO test rig chamber due to the higher energy request of the optical techniques at high-pressure combustion, **Figure 1.b**. The optical system was placed on a remotely controlled translation stage and this allowed to obtain soot and soot precursors cartographies of the entire combustion chamber simultaneously.

2.2 Optical setup

The LII/LIF experimental configuration installed on the academic burner is shown in **Figure 2.a**. The excitation source is a Quanta-Ray pulsed Nd:YAG laser from Spectra Physics. The laser has two fundamentals at 1064 nm, lasing at 12 Hz with a pulse duration of 6 ns at FWHM. One fundamental is used for the LII while the other fundamental is passing through a second harmonic generator (SHG), which induces 532 nm used for LIF. Different configurations of the laser light polarization direction can be selected. The maximum energy/pulse is 850 mJ/pulse for 1064 nm and 300 mJ/pulse for 532 nm for a laser beam diameter of 9 mm. The laser beam profile is Gaussian in the near field and it can be easily shaped for long-distance applications. 1064 nm wavelength is used for inducing the LII signal and 532 nm is used for inducing the LIF signal only. The Gaussian beam is shaped into a 'top-hat' profile using a system of negative and positive cylindrical and spherical lenses. The laser sheet generator contains a negative cylindrical lens with f=-10 mm, an afocal system composed of two spherical lenses and a positive cylindrical lens with f=1000 mm. This optical configuration converts the Gaussian laser beam into a laser sheet having 14 cm height and 0.3 mm width. The waist of the Gaussian beam is almost constant over at least 10 cm in the direction of light propagation. The focal point of the laser sheet is set in the center of the burner. The acquisition system collects the induced LII/LIF radiation at 90^0 with respect to the laser beam propagation axis through the flame. The recording of the induced signals is made with a system composed of the following elements: sCMOS camera, intensifier, objective and a hard-coated band pass filter. The sCMOS camera and the intensifier are coupled with a set of relay lenses. The maximum acquisition frequency at the full-frame is 50 Hz. The camera and the intensifier were integrated by Lavision and developed for OH-PLIF measurements. To some extent, the system can be used for LII/LIF measurements in laminar flames. The size of the sCMOS camera sensor is 2560 x 2160 pixels. The time for recording one image is between 0.5 to 100 ms; this information is essential for the subtraction of the flame emission from the induced signal. The image intensifier (intensified relay optics - IRO) is getable and acts as a fast shutter with a minimum exposure time of 10 ns. This intensifier contains a photocathode with a P43 phosphor that limits the interframe time to at least 1 ms to avoid any residual from the afterglow decay time of the initial image. For this reason, this intensifier is not adapted to LII/LIF measurements in turbulent flows because the emission of the flame has to be recorded as close as possible to the image containing the induced signal otherwise, the subtracted signal does not correspond to the instantaneous emission of the flame. A Canon objective with a focal length of 135 mm was used for obtaining a field of view

of 110 mm x 90 mm. The emitted signal was selected with a 10 nm bandpass filter centered at 450 nm. LII configuration was implemented first and LIF tests followed it. The laser sheet generator position changed between LII and LIF measurements due to the difference in the two wavelengths' focal point.
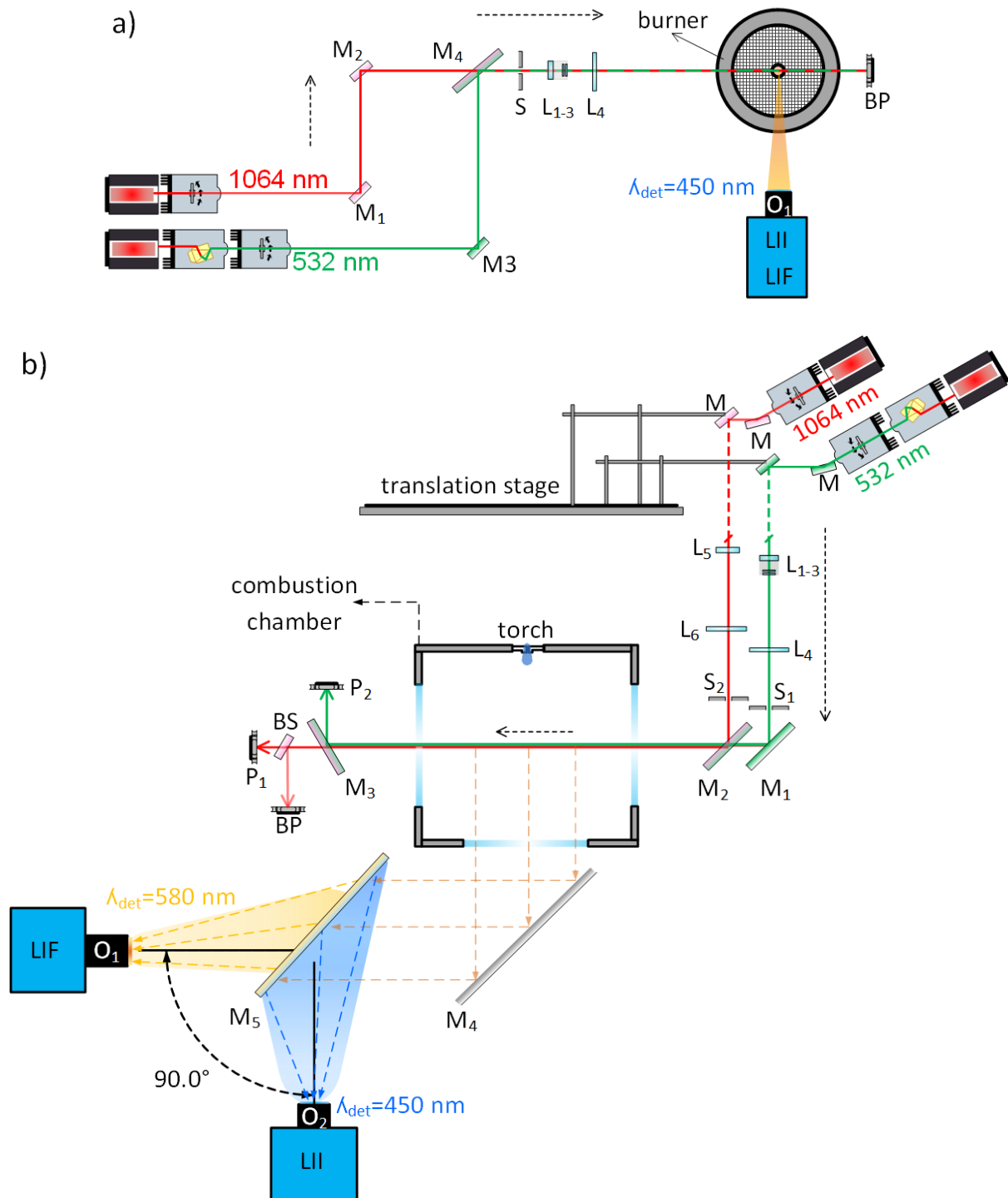

Figure 2.a) Experimental configuration of the LII/LIF techniques installed around the academic burner; **b)** Transversal plan of LII/LIF techniques installed on the combustion chamber of the test rig. L – lens, S – slit, M – mirror, P – power meter, BS – beam splitter, BP – laser beam profiler, F – filter, O – objective, LII/LIF – intensified camera for LII and LIF.

The working principle of the optical setup implemented on the MICADO test rig is similar to the one developed around the academic burner. The degree of complexity increased due to the limited access around the test rig and the remote control of the instruments while the combustor was running. Two lasers are used for the coupled LII/LIF experiments (**Figure 2.b.**). Detailed information about the LII system was presented in Geigle et al.[15]. For LII, the fundamental of a Nd:YAG laser (pulse duration of 7 ns at 10 Hz, Briliant B, Quantel) at 1064 nm is formed into a homogeneous laser sheet by a cylindrical (f=-50 mm) and spherical (f=1000 mm) lens. A 50 mm x 0.2 mm laser sheet was focused on the central axis of the combustor, aligned with the nozzle of the fuel injector. The laser sheet energy on the focus point was 60 mJ/pulse for a surface of 50 mm x 0.2 mm. LII images are recorded perpendicular to the excitation plane with an image intensifier dual-frame CCD camera equipped with Nikon f/2.5 camera lens. The first exposure of 20 ns is used to record the self-emission of the flame and immediately after this (200 ns delay) is recorded the LII signal with the same exposure gate width (GW).

A second Nd:YAG laser coupled to a SHG module resulted in 532 nm wavelength with a pulse duration smaller than 10 ns at 10 Hz (ULTRA CFR200, Quantel). This wavelength is used to induce the selective fluorescence of high molecular classes of PAH. The same laser sheet generator lenses as the one used for the sheet prepared on the academic burner is used in this case. A laser sheet of 60 mm x 1 mm was aligned with the IR laser sheet via a laser beam combiner before the combustion chamber entrance. The pulse energy of 20 mJ was measured on the middle of the chamber for a 50 mm x 1 mm surface at the waist of the laser sheet. The induced fluorescence signal was recorded with a GW of 50 ns after the peak of the laser pulse. The flame emission background image was recorded with the LII camera. A correction algorithm was implemented to account for the different GW exposures and detection wavelength domains between LII and LIF signals.

The LII/ LIF signals are reflected with a high-transmission mirror in the visible domain, below the combustion chamber and send to two camera detectors places at 90^0 one from another. The LIF signal is separated from LII signal with a 500 nm cut-off dichroic mirror. The emission between 400-500 nm wavelength domain is reflected towards the LII camera detector, while emitted wavelengths between 500-750 nm are reflected on the LIF intensified camera. LII and LIF signals were recorded simultaneously with a delay of 1 µs to prevent the two signals' interference. Short bandpass filters were placed in front of the cameras for selecting the LII and LIF signals at the desired wavelength. LII was collected over 50 nm wavelength domain centered at 450 nm and LIF was collected on 10 nm wavelength domain centered at 580 nm. These wavelengths were selected in order to avoid the interference of carbon Swan emission bands at high-pressure combustion conditions. Soot and PAH images were matched to each other based on a standard target image. The simultaneous images recorded with both cameras were flat-field corrected with an image recorded from a homogeneous surface-emission lamp source. This process allows the overlap of the LII/LIF images while avoiding the inhomogeneous response of the pixels of the two cameras.

3 Results and discussion

3.1 Simultaneous detection of soot and precursors on the academic burner

A progressive approach is followed for implementation of the optical techniques, where LII/LIF is first tested and evaluated in a laminar diffusion flame stabilized on a coflow burner at atmospheric pressure. Laboratory flames at atmospheric pressure are studied because it is possible to follow the combustion chemistry and the growth of soot particles along the flame axis, i.e. with the HAB coordinate. Additionally, these flames are of great use for developing and preparing the experimental setup before transferring it to the test rigs. The optical configuration and the working parameters as the laser sheet generation and dimensions, adequate laser fluence for LII and LIF, were evaluated in the CH_4/air flame.

The LII images are obtained for the entire height of the flame and they are representative of the soot region in the laminar CH_4/air diffusion flame. **Figure 3**.3 shows the soot region identified in the selected flame, **Figure 3**.1. Soot particles are present on the edges of the flame at heights above the burner (HAB) located towards the stabilization plate (**Figure 3**.3). Thermal effects can influence the flame near the non-cooled stabilization flame. Therefore the non-desired effects have to be taken into account for long working times of the burner. This soot map is specific to laminar diffusion flames and is a first validation of the LII technique implemented in the laboratory on a laminar diffusion flame at atmospheric pressure.
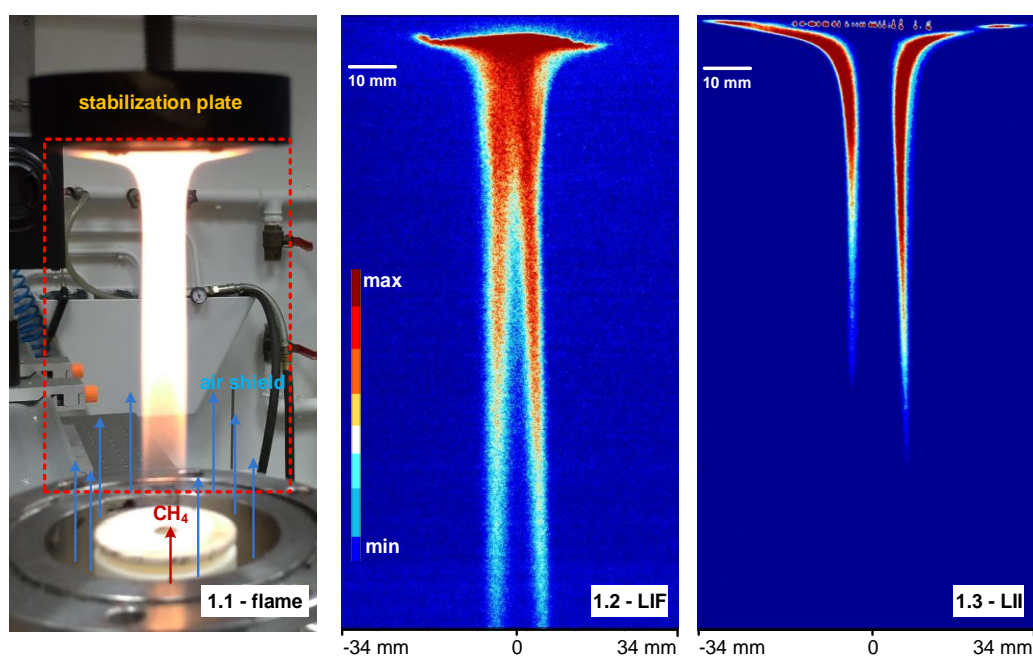

Figure 3.1 The bright zone of the CH_4/air laminar diffusion flame produced by a coflow burner. The field of view of the camera corresponds to the dashed red rectangle, representing the top 8 cm of the flame just below the stagnation plate. **3.2** The LIF signal-induced at 532 nm with a fluence of 0.4 mJ/cm^2. The LII signal is not activated for this fluence setting. **3.3** The LII signal-induced at 1064 nm with 250 mJ/cm^2 fluence. LIF/LII images are collected with a frequency of 12 Hz. The maps correspond to the detection of the induced broadband emission centered at 450 nm (bandwidth of 10 nm), during 50 ns exposure time of the camera intensifier. The images are averaged over 100 laser pulses.

The soot map of the flame is used to select a region of interest (ROI) from the entire flame for obtaining the fluence curves indicative of the sublimation point of "mature" or "young" soot. The fluence curves were obtained for LII emission at 450 nm. The selected values at four HAB are displayed in **Figure 4**. The sublimation threshold is reached at 0.16 J/cm^2 for the selected wavelength domain at the different locations into the flame. Soot particles vaporized after 0.17 J/cm^2 in these combustion conditions when using a Gaussian laser sheet. Soot particles with different physicochemical properties than those measured in this case have different sublimation thresholds, dependent on their optical properties. For this reason, it is almost impossible to estimate the optical properties of fractal-like particles in high-pressure combustion chambers. Most of the time, approximations are made for the calibration of the LII signal in soot volume fraction, in which a constant value of $E_m(\lambda)$ is considered.
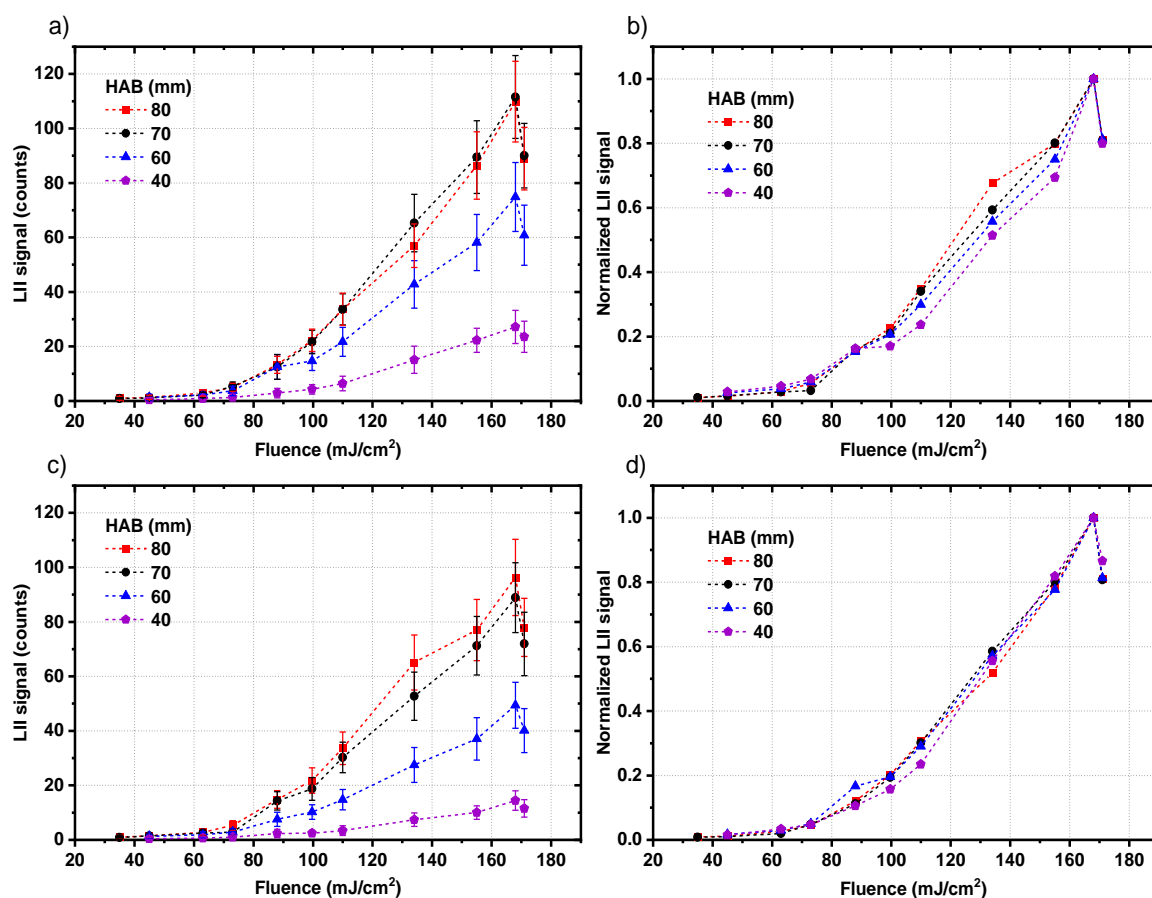
Figure 4 LII fluence curves obtained on the CH$_4$/air laminar diffusion flame. The signal was averaged on a region of interest of 50 x 100 pixels. The curves correspond to four heights above the burner (HAB). A) LII counts subtracted from the right-wing of the flame; b) normalized LII signal from the right-wing of the flame; c) LII counts subtracted from the left-wing of the flame; d) normalized LII signal from the left-wing of the flame.

The synchronization of VIS-LIF with LII is of high interest for unveiling details about the nucleation of soot particles in flames. Therefore the feasibility of the coupling of the two techniques was first tested on this flame. The LIF and LII were performed separately in these cases. Green wavelength (532 nm) was directed through the same optical path as the one used for IR, into the CH$_4$/air burner. The fluorescence signal was recorded at the same emission

wavelength as the LII (450 nm – anti-Stokes detection). The map of soot precursors induced with visible electromagnetic radiation is displayed in **Figure 3.2**. It is well known that 532 nm induces both LII and LIF signals. In this work, it was selected a value of the laser fluence, which did not activate the LII. Some disadvantages of this filtering of the LIF signal can be prominent in high-pressure combustion due to the rapid quenching of the LIF signal and the absorption of the laser radiation in the combustion chamber. A slightly higher fluence was used during the test rig measurements to avoid the laser sheet attenuation across the combustion chamber.

Soot precursors are present in the centerline of the flame near the soot zones, centered with respect to the flame axis near the stabilization plate. The signal from soot precursors is less prominent than that of soot particles because these molecular compounds are participating in soot formation (**Figure 3**) and due to the anti-Stokes detection wavelength domain. It is of high interest to detect these predictors of soot particles' formation zones in aeronautic combustors.

3.2 Simultaneous detection of soot and precursors on the MICADO test rig

Three selected working points for the MICADO test rig are presented in this work. Each WP has a particularity regarding the combustion conditions. A summary of the tested WP in terms of the total mass of air, the air temperature, and the pressure in the combustion chamber are shown in **Figure 5**. The selected WP correspond to the green dots on the graph.
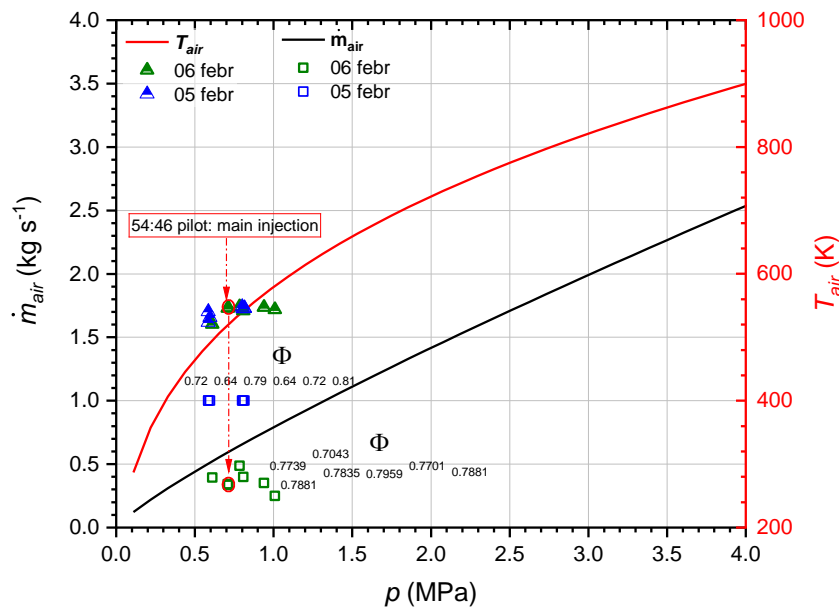

Figure 5. Combustion conditions tested on the MICADO test rig during the SOPRANO measurement campaign. The total mass of injected air and the specific temperature are represented as a function of the pressure in the combustion chamber. Blue points correspond to the first tested WP and green points correspond to the second WP measurements. Temperatures are represented by a triangular shape, while the total mass of air is represented by a square shape.

WP1 is characterized by a low equivalence ratio of the combustion, with a pilot injection for the kerosene. The equivalence ratio is increased for WP2, when the pilot injection is maintained. Pilot and main injection are used for WP3.

Cartographies of soot particles and soot precursors were obtained after two measurements, one near the injector (p1) and a second one towards the bottom of the chamber

(p2). LII was detected at 450 nm, while LIF was detected at 580 nm (Stokes detection). Instantaneous recordings for the three working points are presented in **Figure 6**. LII and LIF cartographies are distinctive for the selected WP. It is observed an increase in the soot volume fraction from WP1 to WP2. This increase in the soot volume fraction is due to the insufficient oxidant for a better combustion. The soot volume fraction increased from 0.08 ppm at WP1 to 1.2 ppm at WP2. The mixing of pilot and main injection reduced the overall contribution of the soot volume fraction to 0.16 ppm.
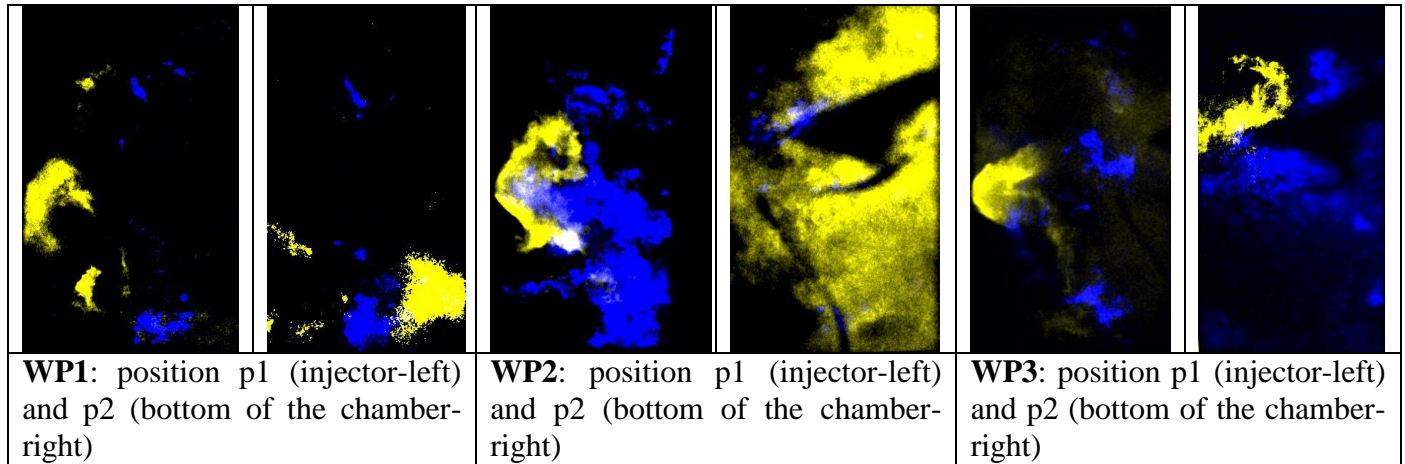

| **WP1**: position p1 (injector-left) and p2 (bottom of the chamber-right) | **WP2**: position p1 (injector-left) and p2 (bottom of the chamber-right) | **WP3**: position p1 (injector-left) and p2 (bottom of the chamber-right) |

Figure 6. Instantaneous recordings of LIF (yellow color) and LII (blue color) were obtained at 10 Hz with 20 ns and 50 ns exposure time and a delay of 1 µs between the laser pulses of the two techniques.

Soot precursors zones are detected mostly near the injector for WP1 and WP3. On the other hand, the aromatic compounds' distribution is predominant in the entire chamber for WP2. There is a linear correlation between the LII and LIF signals. LIF signals can be attributed to high mass PAH, but recently, it was shown that this signal could correspond to covalently bonded dimers of aromatic compounds with the number of rings between two and four[27,28]. Additional studies have to be performed for finding the culprit fluorescent PAH induced with visible wavelengths in harsh combustion conditions due to the significant contribution of the quenching on the LIF signal and the excitation of the "hot emission" bands of PAH.

The presented results have great potential in predicting better values of the heat transfer rates and the interaction near the wall of the combustion chamber. Additionally, the data can validate theoretical models and significantly narrow down the mechanisms participating in the formation of particles in aeronautic combustion chambers. Optical techniques as particle image velocimetry or the PLIF OH can bring valuable information on the presented data.

4   Conclusions

This study presented the step-by-step implementation and development of laser-induced incandescence and laser-induced fluorescence to study soot particle formation in a semi-technical aeronautic test rig. A first validation of the coupled LII/LIF was performed on a laboratory flame. This allowed the translation of the optical setup on the MICADO test rig. A successful measurement campaign was possible due to the collaboration of DLR (responsible of LII measurements) and ONERA (responsible of the LIF measurements and test rig operation). Results obtained in three working points were presented in this work. There is a

direct correlation between the fluorescence of polycyclic aromatic compounds and soot volume fractions detected in the combustion chamber at pressure values between 0.7 and 1 MPa. These large molecular gas-phase compounds play a crucial role in the mechanisms involved in the nucleation of soot particles and this is why their detection is of high interest. The distribution of soot and precursors gives information about the evolution of the kinetics of soot at different instants and working parameters of the combustor. This study goal is in line with the European directives and regulations regarding particulate and gaseous emissions from commercial airplanes.

References

1. ICAO. http://www.icao.int/Pages/default.aspx.

2. Koelmans, A. A. *et al.* Black carbon: The reverse of its dark side. *Chemosphere* **63**, 365–377 (2006).

3. Highwood, E. J. & Kinnersley, R. P. When smoke gets in our eyes: The multiple impacts of atmospheric black carbon on climate, air quality and health. *Environ. Int.* **32**, 560–566 (2006).

4. Jacobson, M. Z. Short-term effects of controlling fossil-fuel soot, biofuel soot and gases, and methane on climate, Arctic ice, and air pollution health. *J. Geophys. Res. Atmos.* **115**, (2010).

5. Bond, T. C. *et al.* Bounding the role of black carbon in the climate system: A scientific assessment. *J. Geophys. Res. Atmos.* **118**, 5380–5552 (2013).

6. Pontius, F. W. & Pontius, N. L. *Drinking water contaminant candidate list released. Journal / American Water Works Association* vol. 90 (1998).

7. Hoek, G. *et al.* Long-term air pollution exposure and cardio- respiratory mortality: a review. *Environ. Heal.* **12**, 43 (2013).

8. Mansurov, Z. A. Soot formation in combustion processes (review). *Combust. Explos. Shock Waves* **41**, 727–744 (2005).

9. Cesaroni, G. *et al.* Long-term exposure to urban air pollution and mortality in a cohort of more than a million adults in Rome. *Environ. Health Perspect.* **121**, 324–331 (2013).

10. Paoli, R., Nybelen, L., Picot, J. & Cariolle, D. Effects of jet/vortex interaction on contrail formation in supersaturated conditions. *Phys. Fluids* **25**, 053305 (2013).

11. Giusti, A. & Mastorakos, E. Turbulent Combustion Modelling and Experiments: Recent Trends and Developments. *Flow, Turbul. Combust.* **103**, 847–869 (2019).

12. Hassanaly, M. & Raman, V. Computational tools for data-poor problems in turbulent

combustion. *AIAA Scitech 2019 Forum* (2019) doi:10.2514/6.2019-0998.

13. Tsurikov, M. S. *et al.* Laser-based investigation of soot formation in laminar premixed flames at atmospheric and elevated pressures. *Combust. Sci. Technol.* **177**, 1835–1862 (2005).

14. Massey, J. C., Chen, Z. X. & Swaminathan, N. Lean Flame Root Dynamics in a Gas Turbine Model Combustor. *Combust. Sci. Technol.* **191**, 1019–1042 (2019).

15. Geigle, K. P., O'Loughlin, W., Hadef, R. & Meier, W. Visualization of soot inception in turbulent pressurized flames by simultaneous measurement of laser-induced fluorescence of polycyclic aromatic hydrocarbons and laser-induced incandescence, and correlation to OH distributions. *Appl. Phys. B Lasers Opt.* **119**, 717–730 (2015).

16. Chatterjee, S. & Gülder, Ö. L. Soot concentration and primary particle size in swirl-stabilized non-premixed turbulent flames of ethylene and air. *Exp. Therm. Fluid Sci.* **95**, 73–80 (2018).

17. Kohse-Höinghaus, K. Combustion in the future: The importance of chemistry. *Proc. Combust. Inst.* (2020) doi:10.1016/j.proci.2020.06.375.

18. Stöhr, M. *et al.* Time-resolved study of transient soot formation in an aero-engine model combustor at elevated pressure. *Proc. Combust. Inst.* **37**, 5421–5428 (2019).

19. Cochet, A. *et al.* Issue 11-June 2016-ONERA test facilities for Combustion in Aero Gas Turbine Engines Challenges in Combustion for Aerospace Propulsion ONERA test Facilities for Combustion in Aero Gas Turbine Engines, and Associated Optical Diagnostics. doi:10.12762/2016.AL11-01.

20. Orain, M., Baranger, P., Ledier, C., Apeloig, J. & Grisch, F. Fluorescence spectroscopy of kerosene vapour at high temperatures and pressures: Potential for gas turbines measurements. *Appl. Phys. B Lasers Opt.* **116**, 729–745 (2014).

21. Eberle, C., Gerlinger, P., Geigle, K. P. & Aigner, M. Toward finite-rate chemistry large-eddy simulations of sooting swirl flames. *Combust. Sci. Technol.* **190**, 1194–1217 (2018).

22. Irimiea, C. *et al.* Unveiling trends in soot nucleation and growth : When secondary ion mass spectrometry meets statistical analysis. *Carbon N. Y.* **144**, 1–16 (2019).

23. Delhaye, D. *et al.* The MERMOSE project: characterization of particulate matter emissions of a commercial aircraft engine. *J. Aerosol Sci.* **105**, 48–63 (2016).

24. Stone, R., Williams, B. & Ewart, P. Optical Techniques that can be Applied to Investigate GDI Engine Combustion. *SAE Tech. Pap.* **2017**-**Septe**, (2017).

25. Geigle, K. P. *et al.* Investigation of soot formation in pressurized swirl flames by laser measurements of temperature, flame structures and soot concentrations. *Proc. Combust. Inst.* **35**, 3373–3380 (2015).

26. SOPRANO project. http://www.soprano-h2020.eu/.

27. Mercier, X., Carrivain, O., Irimiea, C., Faccinetto, A. & Therssen, E. Dimers of polycyclic aromatic hydrocarbons: The missing pieces in the soot formation process. *Phys. Chem. Chem. Phys.* **21**, 8285–8294 (2019).

28. Faccinetto, A. *et al.* Evidence on the formation of dimers of polycyclic aromatic

hydrocarbons in a laminar diffusion flame. *Commun. Chem.* **3**, (2020).

29. Bejaoui, S., Mercier, X., Desgroux, P. & Therssen, E. Laser induced fluorescence spectroscopy of aromatic species produced in atmospheric sooting flames using UV and visible excitation wavelengths. *Combust. Flame* **161**, 2479–2491 (2014).

30. Leermakers, C. A. J. & Musculus, M. P. B. In-cylinder soot precursor growth in a low-temperature combustion diesel engine: Laser-induced fluorescence of polycyclic aromatic hydrocarbons. *Proc. Combust. Inst.* **35**, 3079–3086 (2015).